



Summer oxygen dynamics in the bottom waters of a wide, temperate shelf sea

Xin Meng^{1,2}, Claire Mahaffey¹, Juliane Wihsgott³ and Jonathan Sharples¹

¹School of Environmental Sciences, University of Liverpool, Brownlow Street, Liverpool, L69 3GP, UK

5 ²Department of Geography, University of Exeter, Exeter, EX4 4QE, UK

³Plymouth Marine Laboratory, Prospect Place, Plymouth, PL1 3DH, UK.

Correspondence to: Jonathan Sharples (Jonathan.Sharples@liverpool.ac.uk)

Abstract. Seasonal depletion of dissolved oxygen (DO) in stratified shelf seas has important consequences for benthic and pelagic ecosystems and biogeochemical cycling. There is a need to understand the importance of different processes contributing to the bottom water oxygen budget, and how those processes might change in a warmer ocean. Using CTD observations from the UK Shelf Sea Biogeochemistry programme, we construct a summer DO budget for the bottom waters of the Celtic Sea and use the budget to assess how bottom water DO might change in a warmer climate. Across the shelf, bottom water DO concentration declined during summer stratification, with greater losses in shallow northern waters and slower depletion in deeper southern regions. At a well-sampled site in the central Celtic Sea, the bottom water shows a consistent net DO loss of -44 ± 4 mmol m⁻² d⁻¹. Respiration and remineralization dominate this decline (-54 ± 19 mmol m⁻² d⁻¹), while vertical turbulent fluxes from the subsurface chlorophyll maximum (SCM) form an important DO source (30 ± 17 mmol m⁻² d⁻¹). Episodic wind events enhance DO supply from the SCM, helping to offset some of the DO consumption in the bottom water. Benthic oxygen demand and horizontal transports make minor contributions to the DO budget. A +2 °C “business as usual” climate warming will reduce oxygen solubility and lead to a 12 mmol m⁻³ drop in DO concentration in the bottom water over the summer stratified period. However, we find that increased microbial metabolic rates in the warmer bottom water are more important for changes in bottom water DO concentrations, potentially driving a decrease in DO concentration of about 35 – 66 mmol m⁻³. Combined, these effects will lead to increased oxygen deficiency in the central and northern Celtic Sea. Our results demonstrate the importance of metabolic responses to a warmer ocean, but also the need to better understand changes in winds and wind-driven mixing across the seasonal thermocline.

25

Plain Language Summary. Summer oxygen loss in Celtic Sea bottom waters was investigated using ship observations and an oxygen budget. Seasonal layering cuts deep water off from the air, while microbes breaking down organic matter consume most oxygen. Winds can mix oxygen downward, but warming may worsen oxygen loss by speeding microbial activity and lowering oxygen solubility. This could push parts of the shelf sea toward oxygen deficiency, with risks for seafloor life, and ecosystem health.

30



1 Introduction

Dissolved oxygen (DO) concentrations in the bottom mixed layer of seasonally stratified shelf seas are a sensitive indicator of ecosystem health, biogeochemical cycling, and climate variability (Greenwood et al., 2010). Sustained oxygen depletion can
35 degrade habitat quality, reduce biodiversity and promote the development of hypoxia (Levin et al., 2009). Periods of even modest DO loss, $<190 \mu\text{M}$ compared to saturation concentrations of $250 - 300 \mu\text{M}$, can be deficient for high DO demand organisms such as pelagic and demersal fish (Breitburg, 2002; Diaz and Rosenberg, 2008).

During summer, thermal stratification inhibits vertical mixing, isolating bottom waters from surface DO inputs and atmospheric exchange (Sarma et al., 2016; Rovelli et al., 2016; Sharples et al., 2020). Thus, DO dynamics below the seasonal
40 thermocline are predominantly governed by internal biogeochemical processes and fluxes across the thermocline and benthic boundary layer, though horizontal advection can also play an important role in some shelf sea systems (Sharples et al., 2020; Hull et al., 2020; Rovelli et al., 2016).

Seasonal oxygen depletion has been widely reported in coastal and shelf seas worldwide (Kemp et al., 1992; Breitburg et al., 2018). On the narrow, open shelf off central Oregon, hypoxia arises during upwelling when DO-poor, nutrient-rich waters fuel
45 intense microbial respiration (Adams et al., 2013). In the semi-enclosed North Sea, bottom-water DO saturation commonly drops to 75–80% of saturation values in summer, reflecting organic matter degradation from high surface productivity, and weak vertical exchange between bottom waters and the sea surface (Queste et al., 2013). There is increasing concern that these natural seasonal cycles in bottom water DO are superimposed on a pervasive warming-induced decrease in oxygen solubility, increases in nutrient loading, changes in ocean source waters, and increases in rates of respiration and organic matter
50 degradation (Diaz and Rosenberg, 2008; Schmidtko et al., 2017; Barth et al., 2024; Oschlies et al., 2018).

On the wide, temperate northwest European shelf, the Celtic Sea undergoes strong seasonal stratification from late spring to late autumn. Previous studies have quantified regional DO depletion and identified dominant drivers during the stratified period using moorings and gliders (Hull et al., 2020; Williams et al., 2022). However, a process-based bottom water DO budget spanning the full stratified period remains lacking for the Celtic Sea, and there is a need to better understand how the DO
55 budget might change in a warmer climate. This study assesses the spring-autumn DO environment across the entire Celtic Sea. We construct a detailed DO budget for the bottom waters in the central Celtic Sea and identify the key terms and uncertainties, including wind- and internal wave-modulated mixing between the surface and bottom waters. We also consider how the DO budget in sub-thermocline waters may change in the future as the Celtic Sea warms, altering oxygen solubility, wind-driven mixing and respiration rates, with implications for benthic and pelagic ecosystems.

60 2 Methods

2.1 The Celtic Sea and data availability



The Celtic Sea is a semi-enclosed region of the northwest European shelf (Figure 1a). Stratification begins in spring (April) when net surface heating exceeds mixing by wind and tides (Wihsgott et al., 2019), triggering the spring phytoplankton bloom across the entire region (Seguro et al., 2019; Hopkins et al., 2021). During the stratified period, typically from spring to late autumn, the BML are separated from surface waters by a thermocline. The seasonal thermocline supports the subsurface chlorophyll maximum (SCM; (Sharples et al., 2001) – a site of active photosynthesis and DO production (Rippeth et al., 2024). This seasonal thermocline plays a central role in controlling DO dynamics by isolating deeper waters from atmospheric inputs. Stratification weakens towards the edge of the shelf because of vigorous internal tide mixing (Sharples et al., 2007). We use CTD profiles from a transect across the Celtic Sea (Fig. 1), carried out during the UK Shelf Sea Biogeochemistry research programme over a series of research voyages between March 2014 and August 2015 (Sharples et al., 2019), to provide cross-shelf gradients in the seasonality of bottom water DO concentrations. CTD oxygen sensors were calibrated against DO analyses of discrete water samples (Winkler, 1888) with a typical measurement uncertainty better than $\pm 3 \mu\text{M}$. The number of CTD stations sampled along the transect in Fig. 1 varied, depending on cruise timing and weather conditions. The locations and timing of the CTD sampled stations are reported in Results.

75

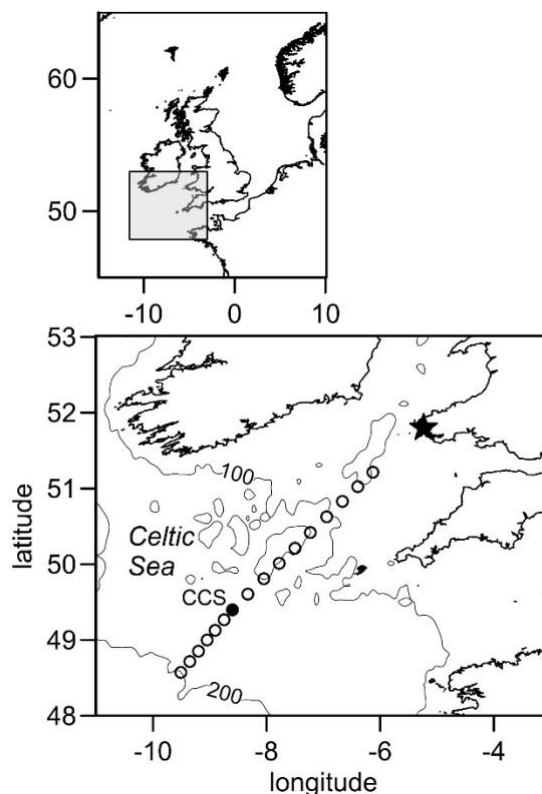


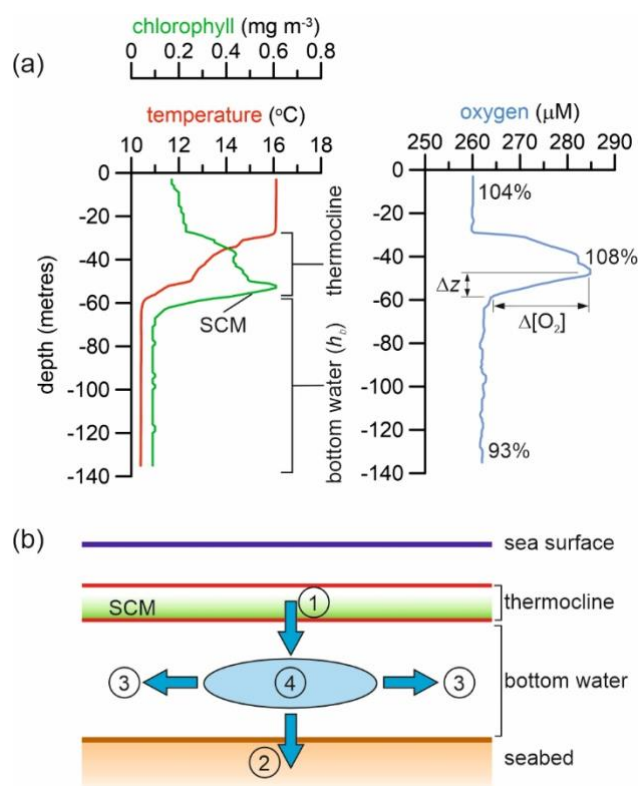
Figure 1. Location of the Celtic Sea study area. Open circles are CTD stations. The filled circle is the central Celtic Sea (CCS) site used for the DO budget. The filled star is the 0 km reference point for transect plots, consistent with Ruiz-Castillo et al. (2019). The 100 and 200 metres isobaths are shown: the shelf edge is marked by the 200 metre isobath.



80 **2.2 DO budget**

One station in the central Celtic Sea (CCS, Fig. 1) was visited during every research voyage, allowing a budget of bottom water DO dynamics to be constructed for this site.

A typical CTD profile at CCS (Fig. 2a) illustrates the vertical structure of the water column during the summer stratified conditions. A warm surface layer is separated from deeper, cold water by a thermocline. The thermocline was identified as the
 85 layer of strong temperature gradient between the much more homogeneous surface and bottom waters (Fig. 2a). The SCM is a persistent feature of the thermocline. DO in the surface waters is close to saturation, but at a lower concentration than colder, deeper waters due to the temperature dependence of solubility. DO in the SCM shows a marked peak because of photosynthesis in the SCM combined with weak diapycnal mixing inside the thermocline which allows the DO to accumulate. Here, we focus on the factors that control the DO concentration in the bottom water. The terms considered in the summer bottom water DO
 90 budget are illustrated in Fig. 2b.



95 **Figure 2.** Typical summer temperature ($^{\circ}\text{C}$), chlorophyll (mg m^{-3}) and DO (μM) profiles at the CCS site indicating the thermocline, bottom water and subsurface chlorophyll maximum (SCM) [14th July 2015 cruise DY033 CTD 08]. On the DO profile the percentages note the saturation state of DO compared to water at the *in situ* temperature and salinity. Key terms in the DO budget: ① diapycnal mixing of DO out of the SCM; ② benthic DO demand; ③ horizontal transports; ④ DO consumption by respiration and organic matter remineralisation.



2.3 Diapycnal DO flux from the SCM

The diapycnal flux of DO across the thermocline, F_{dia} [$\text{mmol m}^{-2} \text{s}^{-1}$] can be calculated from:

$$F_{dia} = -K_z \frac{\Delta[\text{O}_2]}{\Delta z} \quad (1)$$

where K_z ($\text{m}^2 \text{s}^{-1}$) is the vertical turbulent diffusivity. The vertical gradient of DO across the thermocline, $\Delta[\text{O}_2]/\Delta z$ (mmol m^{-4}), was calculated as the difference between the peak DO concentration at the SCM and the DO concentration at the base of the thermocline (Fig. 2a).

Typical values of thermocline turbulent diffusivity in the seasonally stratified Celtic Sea range from 4×10^{-5} to $2 \times 10^{-4} \text{m}^2 \text{s}^{-1}$, reflecting mixing during average summer wind speeds of 5 to 10 m s^{-1} and away from energetic internal waves set up by steep seabed topography (Palmer et al., 2008; Tweddle et al., 2013). For this study we use a representative value of $K_z = 8 \times 10^{-5} \text{m}^2 \text{s}^{-1}$ to compute mean summer DO fluxes, consistent with background diffusivity measurements in the Celtic Sea away from topographic mixing hotspots and strong wind events. The effects of episodic strong wind events on thermocline mixing and DO fluxes are considered separately below.

We include an estimate of the impacts of episodic strong wind mixing events which can significantly augment turbulent diffusivity. Observations by Williams et al. (2013) have shown that sharp pulses of thermocline mixing occur in response to increased winds. Daily mean nitrate fluxes into the base of the SCM increased by a factor of 17 to 22 as winds increased to $>12 \text{m s}^{-1}$. Most of this increase was due to changes in K_z and so this wind-driven increased mixing will also transfer DO from the SCM into the bottom water (Rippeth et al., 2024). Wind events need to be strong enough and sustained for long enough to set up the large-scale inertial motions of the surface layer that are responsible for shear-generated mixing in the thermocline (Burchard and Rippeth, 2009; Lincoln et al., 2016). Based on the observations of Williams et al. (2013), we set a threshold wind speed of 12m s^{-1} sustained for at least 12 hours. When a wind event exceeds this threshold, we increase the thermocline K_z by a factor of 20 (the average increase observed by Williams et al. (2013) and incorporate this into the mean diffusivity over the stratified period. We use hourly wind speed data from the European Centre for Medium Range Weather Forecasting (ECMWF) ERA5 reanalysis (Hersbach et al., 2018) over the stratified periods of 2014 and 2015 at the location of CCS. If the total number of days of stratification between spring and winter is N_s , and the number of days experiencing strong wind events over this period is N_w , then the mean K_z over the stratified period is calculated using:

$$K_z = 8 \times 10^{-5} \times \left[\frac{20N_w + (N_s - N_w)}{N_s} \right] \quad (2)$$

2.4 Benthic DO demand



125 Benthic DO consumption, F_{ben} , was represented using measurements from muddy and sandy sediments, comparable to those at CCS, collected during May (post spring bloom) and August (Hicks et al., 2017). Mean DO consumption rates in sandy sediments (site G) were $-5.9 \pm 2.5 \text{ mmol m}^{-2} \text{ d}^{-1}$ (May: $-6.3 \pm 1.4 \text{ mmol m}^{-2} \text{ d}^{-1}$; Aug: $-5.4 \pm 3.7 \text{ mmol m}^{-2} \text{ d}^{-1}$, Hicks et al. (2017). In muddy sand sediments (site H), mean DO consumption rates were $-9.1 \pm 3.3 \text{ mmol m}^{-2} \text{ d}^{-1}$ (May: $-9.1 \pm 4.0 \text{ mmol m}^{-2} \text{ d}^{-1}$; Aug: $-9.1 \pm 3.3 \text{ mmol m}^{-2} \text{ d}^{-1}$). Using this data set, we have applied a mean of $-7 \pm 3 \text{ mmol m}^{-2} \text{ d}^{-1}$.

130 2.5 Horizontal transport and dispersion

Horizontal transport integrated over the thickness of the bottom water, F_H , was represented as the combined effect of advection and horizontal diffusion operating on cross-shelf gradients in bottom-water DO concentration:

$$F_H = F_{adv} + F_{diff} \quad (3)$$

The horizontal advective flux, F_{adv} , was calculated from:

$$135 \quad F_{adv} = -\bar{v} \frac{\Delta[O_2]}{\Delta y} h_b \quad (4)$$

where y is the cross-shelf direction which is aligned with key physical and biogeochemical gradients (Ruiz-Castillo et al., 2019). The thickness of the bottom layer is h_b (Fig. 2a) and \bar{v} is the mean bottom water cross-shelf current velocity in summer of 0.6 to 0.8 km d^{-1} (Ruiz-Castillo et al., 2019). The horizontal diffusive flux, F_{diff} , was calculated using a horizontal eddy diffusivity K_H in the range 20 to $100 \text{ m}^2 \text{ s}^{-1}$, consistent with values for sub-mesoscale processes on continental shelves
140 (Okubo, 1971), with the horizontal DO gradient:

$$F_{diff} = K_H \frac{\Delta^2[O_2]}{\Delta y^2} h_b \quad (5)$$

2.6 Total respiration demand for DO

Our estimate of the bottom water total respiration demand for DO during the summer, R_{O_2} , is calculated as the residual DO change after diapycnal mixing, benthic DO demand, and horizontal transports have been accounted for in the observed total
145 DO reduction, F_{total} :

$$\begin{aligned} F_{total} &= R_{O_2} + F_{dia} + F_H + F_{ben} \\ R_{O_2} &= F_{total} - F_{dia} - F_H - F_{ben} \end{aligned} \quad (6)$$



3 Results

3.1 Cross-shelf patterns in DO

The cross-shelf pattern of the surface-bottom temperature difference (Fig. 3a) illustrates the expected seasonal variability in stratification. Note in Fig. 3 that there are no data through the middle of winter 2014/15. However, mooring data at CCS confirm that the region was fully mixed vertically by late December 2014 and remained mixed until early April 2015 (Wihsgott et al., 2019). Stratification in the Celtic Sea typically develops in spring (April), intensifies through summer, and peaks in July–August with surface–bottom temperature differences exceeding 9 °C at mid-shelf (~350 km; Fig. 3a). By winter (November–December), the temperature difference rapidly decreases as the water column becomes fully mixed, a state that persists until the following spring. This seasonal cycle was consistent throughout both study years and is a common feature of Celtic Sea seasonality.

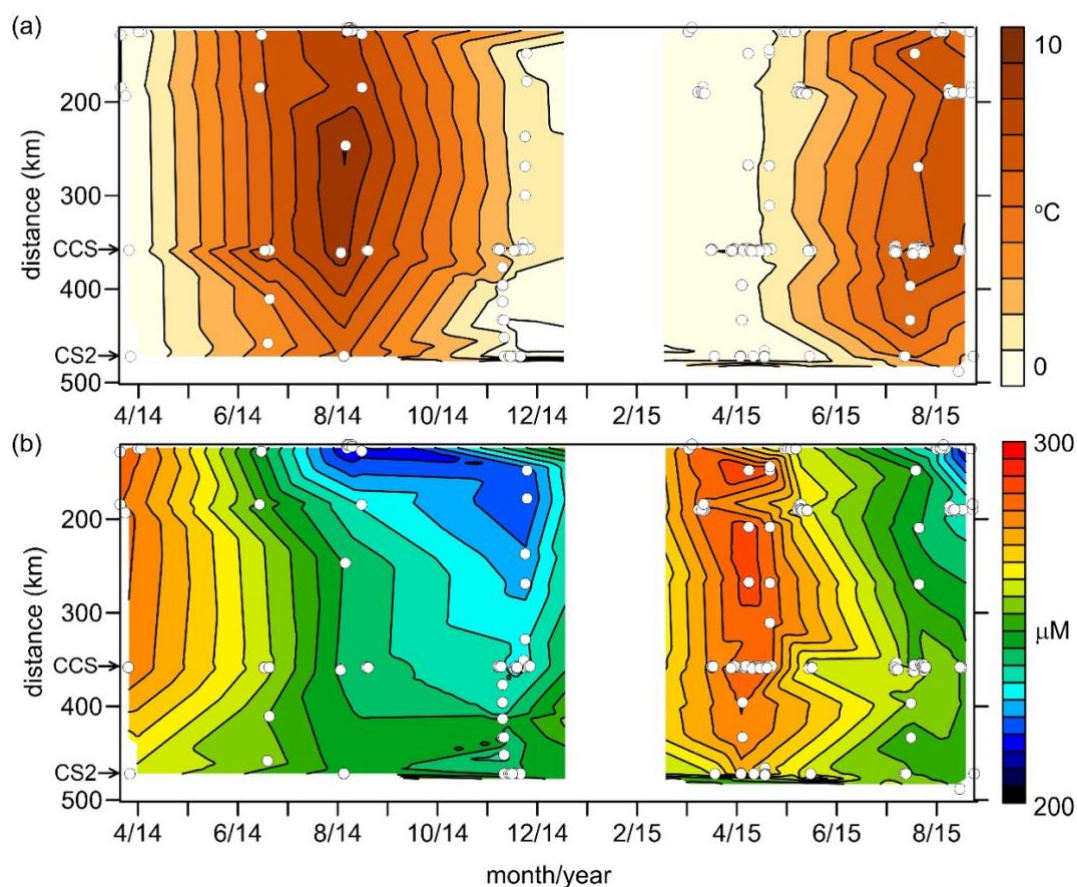


Figure 3. (a) Surface–bottom temperature difference (°C) and (b) bottom mixed layer DO (mmol m^{-3}) along the Celtic Sea transects, April 2014–August 2015. White circles are CTD stations. Distances are relative to the 0 km reference point in Fig. 1.

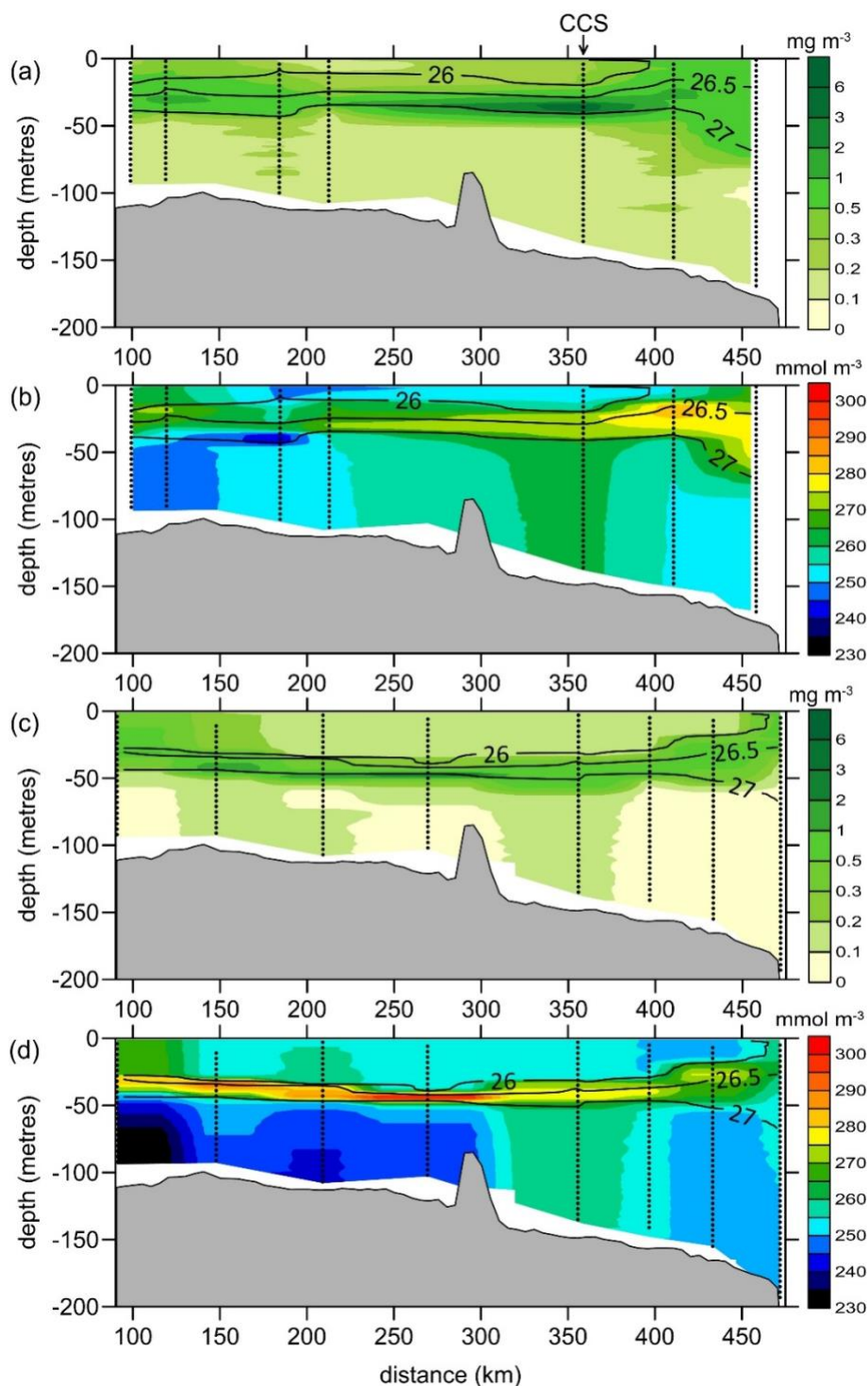
Bottom water DO concentrations show a seasonal cycle closely coupled to the stratification (Figure 3b). DO begins to decline soon after stratification establishes in April, with the steepest losses during peak summer. The lowest DO concentrations (<220



mmol m⁻³) occur in shallower northern areas, while deeper southern waters retain higher DO (e.g. CS2 at the edge of the continental shelf). This spatial gradient reflects both the greater thickness of the bottom layer in deeper regions and, close to the internal tide influenced shelf edge, more efficient ventilation. In winter, when the water column is fully mixed, DO concentrations recover to well-oxygenated conditions (>280 mmol m⁻³) across the transect. The strong correspondence between stratification intensity and DO decline highlights the central role of isolation of bottom waters in driving summer oxygen depletion.

Stratification reaches across the shelf in both summers (Fig. 4), with low surface chlorophyll and a SCM in the base of the pycnocline (Fig. 4a, c). Surface waters are close to 100% saturated, with the lower surface DO concentrations in 2014 associated with a thinner, warmer surface layer (Fig. 4b, d). There is a consistent DO maximum within the pycnocline across the entire shelf, caused by photosynthesis in the SCM combined with weak pycnocline mixing limiting the removal of DO from the SCM. Towards the shelf edge stratification weakens due to mixing by strong internal tides (Sharples et al., 2007). Bottom water DO concentrations (Fig. 4b, d) are minimum in shallower northern waters and increase progressively towards deeper southern regions. For a given areal DO loss from bottom water, a thicker bottom layer experiences a smaller concentration decrease (Große et al., 2016).

The otherwise increasing trend of bottom water DO across the shelf is interrupted in both years by a local peak in DO below the pycnocline near station CCS (Fig. 4b, d), which in 2015 is also associated with an increase in bottom water chlorophyll (Fig. 4c). Horizontally patchy increases in SCM have been noted previously in high-resolution transects across the Celtic Sea out to a depth of about 150 metres and attributed to localized increases in internal mixing associated with variability in seabed slopes (Sharples et al., 2013). The patch of high bottom water DO will not be linked to the obvious bank on the seabed, 50 km away; there are numerous seabed features across the shelf that could drive this elevated mixing (e.g. Sharples et al. (2013)) and it is likely that there are seabed features adjacent to the CTD transect responsible for this localized oxygen increase. We will discuss the implications of this patch of bottom water oxygen for our oxygen budget later.



185 **Figure 4.** Cross-shelf transects during June 2014 (cruise JC105) and July 2015 (cruise DY033). (a) chlorophyll (mg m^{-3}) June 2014; (b) DO (mmol m^{-3}) June 2014; (c) chlorophyll (mg m^{-3}) July 2015; (d) DO (mmol m^{-3}) July 2015. Black contours indicate potential density (σ_θ , kg m^{-3}), and the vertical dotted lines mark the CTD profiles. Distances are relative to the 0 km reference point in Fig. 1.

3.2 Seasonality in the central Celtic Sea

At the CCS site, mooring data illustrates the repeating seasonal cycle of stratification with spring stratification beginning in early April of 2014 and 2015 and winter mixed conditions from mid-December 2014 through to April 2015 (Fig. 5). Chlorophyll from CTD profiles indicates the sub-surface chlorophyll maximum in summer 2014 and 2015, an autumn/fall bloom in surface waters in November 2014 and a strong spring bloom in April 2015 (Fig. 5a). Note that the 2014 spring bloom was not sampled by CTD casts but it was seen in surface waters from the mooring data (Wihsgott et al., 2019). The impact of photosynthesis on DO is clear during the 2015 spring bloom, the 2014 autumn/fall bloom and in the summer sub-surface chlorophyll maximum (Fig. 5b). Again, the lack of CTD data in April and May 2014 means that the DO signal linked to the 2014 spring bloom was not sampled.

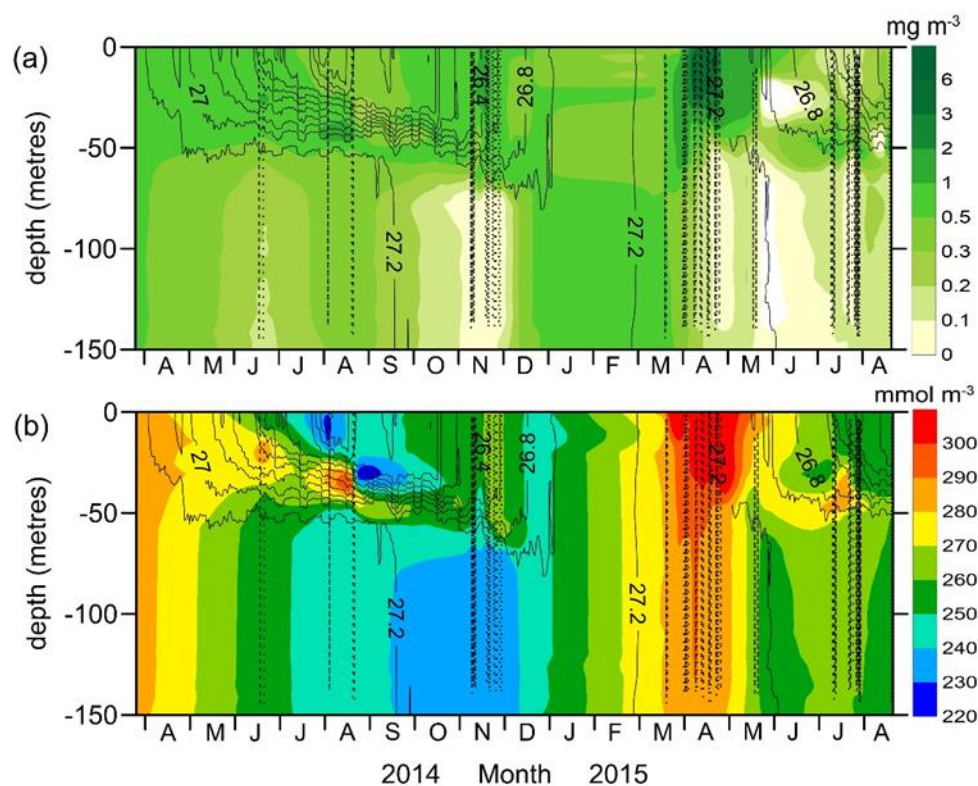
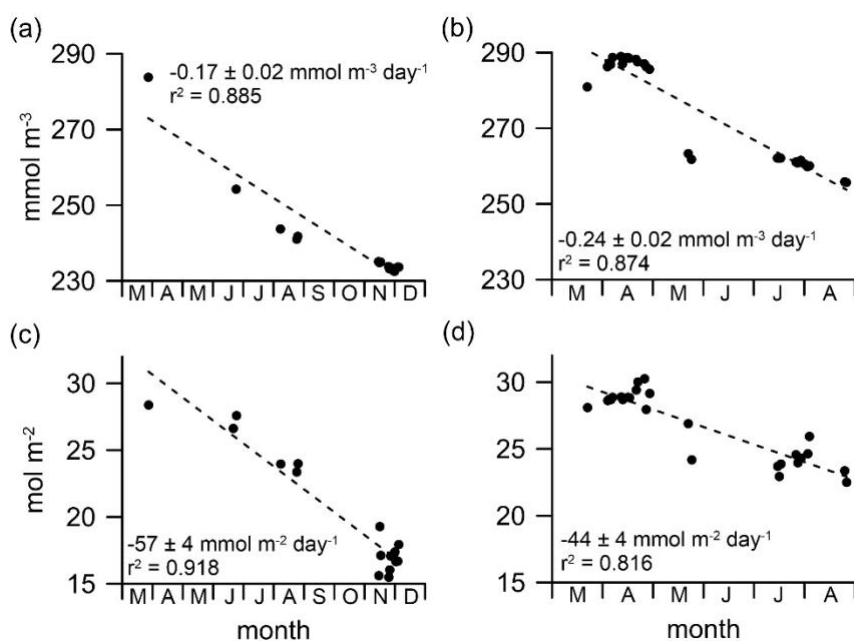


Figure 5. The concentration of (a) chlorophyll (mg m^{-3}) and (b) DO (mmol m^{-3}) at CCS from March 2014 to August 2015. Black contours indicate potential density (σ_θ , kg m^{-3}) using mooring data from Wihsgott et al. (2019). The black dots mark the CTD profiles.

Bottom water DO in March 2014 and March 2015 started at about 282 mmol m^{-3} and was 100% saturated at a water temperature of about $10 \text{ }^\circ\text{C}$. This sets the initial bottom water DO concentration at the start of the stratified period. In April 2015 there was a slight increase in DO following the spring bloom, reaching 288 mmol m^{-3} ; most likely the result of spring tide ventilating the BML with high DO surface water containing the spring bloom. In both summers DO concentrations declined over the stratified period, to minimum concentration of 230 mmol m^{-3} in late November 2014 (Figure 5b).



205 DO concentrations in bottom waters declined at a rate of $0.17 \text{ mmol m}^{-3} \text{ d}^{-1}$ in 2014 and $0.24 \text{ mmol m}^{-3} \text{ d}^{-1}$ in 2015 (slopes of
the lines in Fig. 6a, b) and are consistent with other measurements in the Celtic Sea (Hull et al., 2020; Williams et al., 2022).
At a site close to the north of our transect line, DO has previously been noted to decline at rates of 0.40, 0.32 and $0.14 \text{ mmol m}^{-3} \text{ d}^{-1}$
in spring, summer and autumn/fall, respectively (Hull et al., 2020). Using glider-based measurements near CCS,
Williams et al. (2022), measured DO decline rates of 0.23 and $0.10 \text{ mmol m}^{-3} \text{ d}^{-1}$ in spring and summer respectively. While
210 our CTD time series do not have sufficient duration or resolution in any one year to determine how rates of decline might
change through the stratified period, the relatively low rate of decrease in late summer/early autumn 2014 and the higher rate
of decrease in early summer 2015 are consistent with the variations seen by Hull et al. (2020), and Williams et al. (2022).



215 **Figure 6. (a) mean DO concentration (mmol m^{-3}) in the lower 40 metres in 2014; (b) mean DO concentration (mmol m^{-3}) in the lower 40 metres in 2015; (c) integrated DO (mol m^{-2}) below the thermocline in 2014; (d) integrated DO (mol m^{-2}) below the thermocline in 2015**

DO inventories below the seasonal thermocline were used in the budget estimates. Mean DO concentrations were calculated
over the lower 40 metres of the water column (Fig.6a,b) as a practical measure of the bottom water DO, while DO inventories
were integrated between the base of the thermocline and the seabed (h_b , Fig. 2a). The inventories show clear declines over
the stratified period (Fig. 6c, d). The rate of decline in 2014 ($-57 \pm 4 \text{ mmol m}^{-2} \text{ d}^{-1}$) was steeper than in 2015 ($-44 \pm 4 \text{ mmol m}^{-2} \text{ d}^{-1}$).
220 However, the 2014 regression will be influenced by the November 2014 surface layer having deepened considerably as
the system approach the fully mixed state (which occurred in late December). Thus, the thickness of the water layer below the
thermocline was reduced to about 70 metres, compared to 100 metres through most of the rest of the stratified period (Fig. 5).



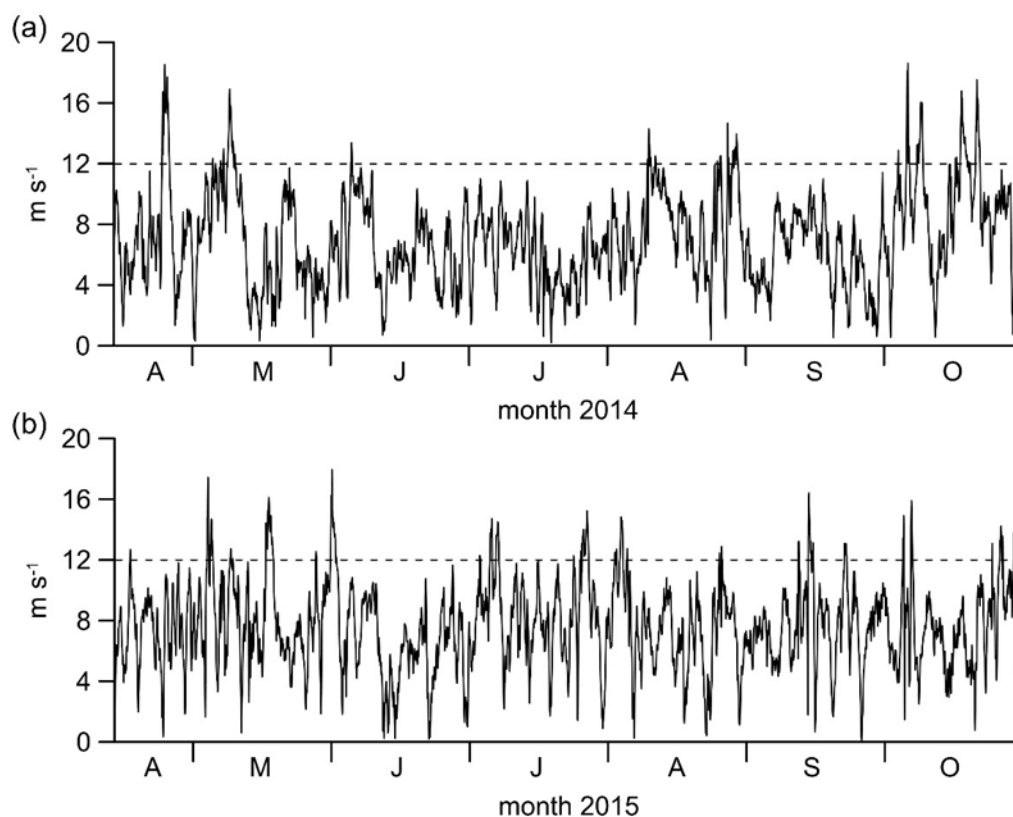
225 The rates of decline from 2015 are more relevant to our budget because they are not affected by entrainment of DO by surface layer deepening.

3.3 DO budget in the Bottom Mixed Layer

230 The mean rate of decline in the bottom water DO at CCS between June and November 2014 and April and August 2015 was used to evaluate the relative contributions of physical and biological processes controlling summer DO dynamics. This net decrease in the bottom water DO inventory reflects the combined influence of benthic consumption, horizontal transports, and vertical mixing acting alongside biological respiration within the sbottom water (Fig. 2b). Our aim here is to achieve a reliable understanding of the relative importance of each process.

3.3.1 Vertical mixing

235 The effect of strong winds on the DO flux from the SCM can now be considered using the wind speed threshold and calculation of K_z described earlier (Eq.(2)). We use a stratified period between mid-April and end October so that $N_S = 200$ days. Beyond October we expect rapid convective deepening from November to dominate any influence of wind-driven mixing. Wind speed data from ERA5 (Fig. 7) illustrates the episodic nature of strong wind events. Analysis using the speed and time thresholds between mid-April and October yields $N_w = 8.3$ days for 2014, and $N_w = 8.6$ days for 2015. Equation. (2) then gives $K_z = 14.3 \times 10^{-5} \text{ m}^2 \text{ s}^{-1}$ for 2014 and $K_z = 14.5 \times 10^{-5} \text{ m}^2 \text{ s}^{-1}$ for 2015. The wind-driven component of the DO budget then combines K_z with the vertical DO gradient from all available CTD profiles within the stratified periods of each of 2014 and 240 2015. The uncertainty in each arises from variability in the DO gradient. Variability caused by the range of mixing enhancements seen by Williams et al. (2013), is only about 10% of the variability caused by the DO gradients and so has not been included. We also consider possible increases in vertical diffusivity that may be caused by nearby seabed features generating enhanced mixing, which earlier we suggested could be responsible for the persistent locally increased DO in the bottom water in summer at CCS. Palmer et al. (2013), measured thermocline diffusivity between 3×10^{-5} (neap tides) and $3 \times 10^{-4} \text{ m}^2 \text{ s}^{-1}$ (spring tides) over the slopes of a bank in the Celtic Sea, with the larger spring tide mixing caused by breaking lee waves on the thermocline. Sections across the Celtic Sea (Sharples et al., 2013) indicate that such topographically driven diapycnal mixing is common across most of the region. Taking the mean of the Palmer et al. (2013) measurements, $1.6 \times 10^{-4} \text{ m}^2 \text{ s}^{-1}$, and adding the wind effect (Eq. (2) using $1.6 \times 10^{-4} \text{ m}^2 \text{ s}^{-1}$ as the background diffusivity) suggests a diffusivity of $2.3 \times 10^{-4} \text{ m}^2 \text{ s}^{-1}$, about 60% greater than our wind-influenced values in the absence of any topographic mixing.



250

Figure 7. ERA5 wind speeds (m s^{-1}) between mid-April and October (a) 2014, (b) 2015 at CCS. The dashed line indicates the wind speed used as the threshold defining a strong wind event.

The results (Table 1) illustrate the importance of including strong wind events, with the average diapycnal DO flux in 2015 being almost doubled compared to a value that uses the canonical shelf sea diapycnal diffusivity. The addition of the effect of enhanced diapycnal mixing caused by topographically driven internal waves suggests that the variability of the shelf seabed should also be considered in an assessment of the diapycnal mixing.

Table 1. Diapycnal DO fluxes for 2014 and 2015 using a vertical diffusivity not incorporating wind events, diffusivity influenced by wind events, and diffusivity influenced by wind events and local topographically-driven mixing.

260

	2014	2015
DO flux (no wind events)	$33 \pm 26 \text{ mmol m}^{-2} \text{ d}^{-1}$	$17 \pm 9 \text{ mmol m}^{-2} \text{ d}^{-1}$
DO flux (including wind events)	$47 \pm 31 \text{ mmol m}^{-2} \text{ d}^{-1}$	$30 \pm 18 \text{ mmol m}^{-2} \text{ d}^{-1}$
DO flux (including wind events and enhanced mixing by local topography)	$76 \pm 49 \text{ mmol m}^{-2} \text{ d}^{-1}$	$47 \pm 29 \text{ mmol m}^{-2} \text{ d}^{-1}$



3.3.2 Horizontal transports

A cross-shelf gradient in bottom-water DO was observed during summer. Along the transect, DO concentration in the bottom water increased from the shallow water toward CCS (from ~ 245 to 260 mmol m^{-3}), then decreased toward shelf edge (from ~ 260 to 250 mmol m^{-3}), creating the local maximum at CCS likely driven by nearby topographically induced mixing (Figure 4b, d). This pattern suggests that horizontal advection and diffusion act as net DO sinks at CCS.

The advective contribution was estimated from the observed horizontal DO gradient ($\sim 1 \times 10^{-4} \text{ mmol m}^{-4}$) and mean near-bottom currents ($\sim 0.6 - 0.8 \text{ km d}^{-1}$), yielding DO changes of -0.06 to $-0.08 \text{ mmol m}^{-3} \text{ d}^{-1}$. Accounting for the water column below the base of the seasonal thermocline, this leads to changes of -5.4 to $-7.1 \text{ mmol m}^{-2} \text{ d}^{-1}$ (mean $-6.3 \pm 0.9 \text{ mmol m}^{-2} \text{ d}^{-1}$). Horizontal eddy diffusion was assessed using a simple 1D model with DO concentration at CCS given an initial Gaussian distribution similar to the CTD observations, with a local maximum in DO concentration set to 10 mmol m^{-3} above the background. Using a range of $K_H = 20 - 100 \text{ m}^2 \text{ s}^{-1}$ (Okubo, 1971), the resulting DO losses ranged from -2.6 to $-10.8 \text{ mmol m}^{-2} \text{ d}^{-1}$ (mean $-6.7 \pm 4.1 \text{ mmol m}^{-2} \text{ d}^{-1}$), similar to the advective estimates.

3.3.3 Benthic demand

Assuming the sediment type at CCS is muddy sand, we estimate mean benthic DO uptake of $-7 \pm 3 \text{ mmol m}^{-2} \text{ d}^{-1}$ (Hicks et al., 2017).

3.3.4 Residual and overall budget

Combining the above DO budget terms (Table 2), the residual DO demand in the bottom water at CCS over the stratified period was estimated at $-84 \pm 32 \text{ mmol m}^{-2} \text{ d}^{-1}$ for 2014 and $-54 \pm 19 \text{ mmol m}^{-2} \text{ d}^{-1}$ in 2015. Remineralisation and respiration in the bottom water are the dominant processes in removing DO, but there is an important resupply of DO through the thermocline that can offset about half of the remineralisation/respiration effect. We view the change in DO in 2014 as less reliable as the CTD sampling in November occurred during a time of rapid deepening of the thermocline as the water column remixed toward December: thus, the bottom layer thickness was reducing which will lead to a decrease in the inventory of DO below the thermocline. The budget in 2015 did not include data beyond the start of September, and so there was a generally consistent bottom layer thickness of 100 m (e.g. Fig. 5). The remineralisation/respiration term calculated for 2015 is higher than the $20 \pm 8 \text{ mmol m}^{-2} \text{ d}^{-1}$ calculated by Williams et al. (2022), but our value is consistent with the $71 \pm 17 \text{ mmol m}^{-2} \text{ d}^{-1}$ measured at CCS by García-Martín et al. (2019).



290 **Table 2. DO budget for the bottom water at CCS during the stratified periods in 2014 and 2015. Circled numbers refer to the processes identified in Fig. 2b. Fluxes in brackets include the effect of topographically driven internal waves as a source of diapycnal mixing.**

Budget term (mmol m ⁻² d ⁻¹)	2014	2015
Total O ₂ change	-57 ± 4	-44 ± 4
① Mixing O ₂ from the SCM	47 ± 31 (76 ± 49)	30 ± 18 (47 ± 29)
② Benthic O ₂ demand	-7 ± 3	-7 ± 3
③ Horizontal advection of O ₂	-6 ± 1	-6 ± 1
③ Horizontal diffusion of O ₂	-7 ± 4	-7 ± 4
④ Respiration and organic matter remineralization of O ₂	-84 ± 32 (-114 ± 49)	-54 ± 19 (-71 ± 29)

4 Discussion

4.1 Key results

CTD observations between March 2014 and August 2015 show a clear seasonal cycle in the bottom water DO concentration, tightly coupled to the development and breakdown of stratification. DO concentrations decline following spring stratification, when isolation from surface exchange limits replenishment. The decline continues through summer, reaching annual minima just before autumnal mixing, consistent with mooring and glider observations in the Celtic Sea (Hull et al., 2020; Williams et al., 2022). Bottom water DO concentrations reach their lowest values in the shallower northern parts of the shelf: thermocline depths are broadly the same across most of the shelf, so shallower regions have a smaller pool of bottom water DO available for respiration and bacterial consumption. Our budget of bottom water DO in the CCS site shows that biological respiration and organic matter remineralisation dominate consumption, with the supply of DO via diapycnal mixing from the high DO concentrations within the SCM providing the next most important budget process. We find that incorporating some measure of the effect of episodic strong wind events on the mixing between the SCM and the bottom water is important. Adding the effect of topographically driven internal waves in enhancing diapycnal mixing also has a significant effect on the final value of oxygen consumption in the bottom waters. Benthic DO demand and horizontal transports contribute only 10 to 15% of the total DO decline.

The oxygen consumption rate for 2014 is certainly an over-estimate, because the starting value of the rate of oxygen loss (the slope in Fig. 6c) will have been steepened by the November CTD data. The bottom layer in November 2014 was significantly thinner (about 75 metres) compared to the more typical 100 metres over most of the stratified period due to the rapid deepening of the surface layer approaching winter. Thus, the November bottom water DO inventory will be bias low. If the 2014 oxygen depletion rate is calculated without the November CTD data, the slope of Fig. 6c would instead be 34 mmol m⁻² d⁻¹, and the



resulting oxygen consumption rate would be $51 \text{ mmol m}^{-2} \text{ d}^{-1}$ (with wind events) or $81 \text{ mmol m}^{-2} \text{ d}^{-1}$ (with wind events and topographic mixing), very close to the 2015 estimates.

Our estimates of consumption are similar to other work in the region. Hull et al. (2020), report value of around $40 \text{ mmol m}^{-2} \text{ d}^{-1}$ at sites in the northern part of our CTD section. Values reported by Williams et al. (2022), for April and July 2015 at CCS are lower at $12 - 29 \text{ mmol m}^{-2} \text{ d}^{-1}$. Williams et al. did not include benthic oxygen demand in their budget and their estimates of horizontal transport of DO are lower than ours. Their estimate of the contribution from diapycnal mixing was significantly lower at $3 - 4 \text{ mmol m}^{-2} \text{ d}^{-1}$. This is mainly because of lower values K_z , between $3 \times 10^{-5} \text{ m}^2 \text{ s}^{-1}$ (April 2015) and $5 \times 10^{-5} \text{ m}^2 \text{ s}^{-1}$ (July 2015), though Williams et al. (2022) did have the advantage of direct measurements of turbulence across the thermocline. Our background $K_z = 8 \times 10^{-5} \text{ m}^2 \text{ s}^{-1}$, along with the wind-induced increases, covers a much longer period April – October with more wind events than seen by Williams et al. (2022), so some discrepancy is perhaps unavoidable. Observations of phytoplankton and bacterial oxygen consumption below the thermocline at CCS made by García-Martín et al. (2019), show total oxygen demand of 50 (July 2015) to 80 (April 2015) $\text{mmol m}^{-2} \text{ d}^{-1}$, very close to our estimates.

4.2 Bottom water DO in a warmer climate

Future warming is expected to exacerbate DO depletion in shelf seas through four mechanisms: reduced oxygen solubility, stronger and longer stratification (Holt et al., 2010), and enhanced microbial respiration (Brewer and Peltzer, 2017). Our analysis also suggests that changes in winds are also an important consideration. Based on the important terms in our DO budget, we now discuss possible changes in DO dynamics in a warmer world. We will focus on the budget terms for 2015, and consider how the bottom water DO inventory and DO concentration will change from the onset of stratification in mid-April through to late October, a total of 200 days of stratification. This avoids the added complexity of the autumn/fall mixing deepening the surface layer and so thinning the amount of water below the thermocline, which will affect the inventory calculation.

4.2.1 Changes in oxygen solubility.

Human-induced warming has already raised global surface temperatures by $\sim 1.1 \text{ }^\circ\text{C}$ above pre-industrial levels and further increases across the NW European shelf of $1.5 - 4 \text{ }^\circ\text{C}$ are projected by 2100 under a “business as usual” climate scenario (SRES A1B; Holt et al. (2010)). We adopt this scenario to allow direct comparison with existing shelf sea projections, acknowledging that it represents an upper bound on future warming. In the Celtic Sea, winter surface waters have already warmed by $0.3 - 0.5 \text{ }^\circ\text{C}$ since the 1990s and are predicted to rise by a further $1.5 - 2.5 \text{ }^\circ\text{C}$ by the end of this century (Holt et al., 2010). Based on this projection we will consider the effect of a temperature rise of $2 \text{ }^\circ\text{C}$ on oxygen solubility.

Surface water temperature in spring, when the water column is still vertically mixed but immediately prior to the onset of seasonal stratification, is critical for assessing oxygen dynamics through the subsequent stratified period. It dictates the water column DO concentration that, when stratification is established and the bottom water is isolated from the atmosphere, provides



the starting point for all processes that alter the DO concentration. At a salinity of 35, and a present-day spring surface temperature of 9°C, the DO concentration at 100% saturation will be 288 mmol m⁻³. A temperature rise of +2.0°C reduces DO to 276 mmol m⁻³, so a reduction of 12 mmol m⁻³. Assuming all DO budget terms are the same as our 2015 calculations, then the DO concentration at the end of October will be 12 mmol m⁻³ lower than in 2015. The oxygen concentration in October 2015 can be estimated by extrapolating the trend in Fig. 6b which yields a concentration of about 237 mmol m⁻³. So, in the warmer climate the change in oxygen solubility alone will lead to a decrease from 237 mmol m⁻³ to 225 mmol m⁻³.

4.2.2 Earlier onset of stratification

In a warmer world it is projected that stratification on the NW European shelf will begin about 5 days earlier than at present (Holt et al., 2010). This will give the DO budget processes an extra 5 days to reduce the BML DO concentration. Assuming the same rates of decline as 2015, then the DO inventory will be lowered by 0.22 ± 0.02 mol m⁻², and the bottom water DO concentration reduced by 2.2 ± 0.2 mmol m⁻³. Earlier onset of stratification therefore has a very minor effect on the bottom water DO dynamics.

4.2.3 Changes in metabolic rates

We will now consider changes to respiration rates in a warmer ocean. Bacterial respiration typically responds to temperature with a Q₁₀ of about 2 (Bendtsen et al., 2015; Laufkötter et al., 2017), while respiration rates of a natural, mixed microbial community in waters similar to the Celtic Sea have a Q₁₀ of about 5 (Lefevre et al., 1994). For a 2°C increase in temperature this suggests a 15 - 38% increase in DO consumption rates, so our 2015 rate of -54 mmol m⁻² d⁻¹ (without topographically-driven diapycnal mixing) becomes -62 to -75 mmol m⁻² d⁻¹. Assuming all other processes have the 2015 rates, then the new net DO depletion rate will be -52 to -65 mmol m⁻² d⁻¹. Starting with the solubility changes in a 2°C warmer ocean, so an initial inventory of 27.6 mol m⁻² and assuming 200 days of stratification from mid-April to the end of October yields an inventory of 14.6 – 17.2 mol m⁻². The bottom water thickness in October 2015 had decreased to about 85 metres, so the inventory changes lead to a near bed DO concentration of 171 - 202 mmol m⁻³. Hence changes in bottom water microbial metabolic rates in a 2°C warmer ocean could reduce the bottom water DO concentration by about 35 – 66 mmol m⁻³. If we view the natural, mixed microbial community as a better model for the community respiration in the bottom waters of the Celtic Sea, then we can expect the additional loss of oxygen in a 2°C warmer ocean to be closer to 66 mmol m⁻³.

4.2.4 Variability in wind events

Finally, given the significance of the wind-mixing term in our DO budget we should consider changes in winds over the region in a warmer world. However, there is no clear consensus on how the number of strong wind events might change over the NW European shelf in response to climate warming, largely because of a wide range of model predictions for latitudinal changes in the Atlantic storm track (Woolf and Wolf, 2013). Instead, we quantify the past long-term variability in the number of



spring/summer strong wind events that meet our thresholds for affecting the mean K_z over the stratified period (Fig. 8). Between 1960 and 2020 there was considerable variability in the contribution of wind events to mean diapycnal diffusivity. The number of days experiencing winds above our event threshold ranged between 1.5 and 20.1 days, with a mean value 10.8 ± 4.1 days. Using the average vertical gradient in DO concentration from mid-April to October 2015 of 2.4 mmol m^{-4} allows us to estimate the changes we might expect in the DO inventory and concentration compared to 2015 (Table 3). The results show that variability in wind events alone could drive changes in September bottom water DO concentrations ranging from $+41 \text{ mmol m}^{-3}$ (maximum wind activity) to -27 mmol m^{-3} (no wind events), highlighting a significant role for interannual wind variability in controlling late summer bottom water DO.

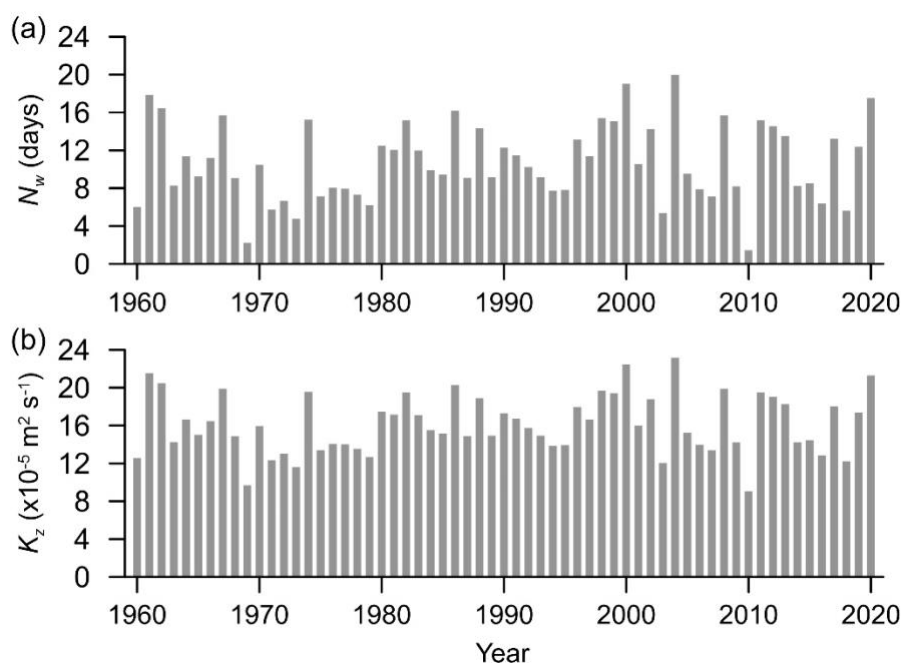


Figure 8. The amount of time experiencing strong wind events (wind speed exceeding 12 m s^{-1} for at least 12 hours) at CCS from 1960 to 2020 during stratified period (mid-April - October). Corresponding mean diapycnal diffusivity during mid-April - October, K_z , based on Eq. (2).

385

Table 3. Variability in mixing and DO impacts caused by changes in the number of wind events. Inventory and concentration changes are relative to the values in 2015. Inventories for 2015 were 28.8 (April) and 20.1 (October) mol m^{-2} with an end October bottom water DO concentration of 237 mmol m^{-3} in a bottom layer thickness of about 85 metres (based on mooring data Fig. 5).

$K_z (\text{m}^2 \text{ s}^{-1})$	DO flux ($\text{mmol m}^{-2} \text{ d}^{-1}$)	Net DO rate ($\text{mmol m}^{-2} \text{ d}^{-1}$)	Change in October inventory (mol m^{-2})	Change in October bottom water DO (mmol m^{-3})
14×10^{-5} (2015)	30	-44	0	0



9×10^{-5} (minimum 1960-2020)	19	-55	-2.2	-27
16×10^{-5} (mean 1960-2020)	33	-41	+0.6	+6
23×10^{-5} (maximum 1960-2020)	48	-26	+3.6	+41

5 Synthesis and conclusions

390 Based on the above analysis we suggest that the dominant process affecting bottom water DO of a temperate shelf sea in a 2°C warmer ocean will be the increase in microbial metabolic rates, leading to a DO reduction in the central Celtic Sea in autumn/fall of about 66 mmol m⁻³. Changes in DO because of reduced solubility in a warmer ocean are significant, at 12 mmol m⁻³, but substantially less than the reduction caused by metabolic rate changes. Changes in DO concentrations caused by an earlier onset of stratification, thus inhibiting the ventilation of the BML for longer, were relatively insignificant, only reducing
395 the DO concentration by about 2 mmol m⁻³.

Changes in bottom water DO caused by episodic strong wind events could be significant. Based on the past variability in winds we find that late summer BML DO concentrations could vary by about +40 to -30 mmol m⁻³. How winds over the NW European shelf might change in a warmer climate is currently uncertain, but the variability we calculate suggests that the effects on DO concentrations could be of a similar magnitude to those arising from solubility and metabolic rate changes. We did not attempt
400 to quantify changes in diapycnal mixing caused by the strengthening of stratification in a warmer ocean or take account of a changing DO gradient across the pycnocline. Reduced mixing across the thermocline may be expected to exacerbate the DO deficit in the bottom water by reducing the mixing of DO downwards from the SCM. However, this simple view of mixing and stratification does not consider changes in the supply of mixing energy into the water column by inertial shear and internal waves, both of which will also respond to changes in the strength of stratification. Also, any reduction in mixing will reduce
405 the supply of nutrients upwards and so reduce primary production and the subsequent supply of organic material to the bottom water: this will decrease the bottom water DO demand.

In a 2°C warmer ocean the combination of greater microbial respiration and decreased oxygen solubility could reduce bottom water DO concentrations by 66+12=78 mmol m⁻³, so an autumn/fall DO concentration of 159 mmol m⁻³. Thus, we find that bottom water DO in the central Celtic Sea could decrease to concentrations below oxygen deficiency, defined as a
410 concentration below 192 mmol m⁻³ (Mahaffey et al., 2023), towards the end of summer. Further north in the Celtic Sea, in shallower water but where we expect broadly the same DO dynamics, the thinner bottom layer means that bottom water DO concentrations are likely to drop further below the oxygen deficiency threshold before the end of the stratified period. Modelled predictions of future DO in the Celtic Sea show reductions of late summer bottom water concentrations by the end of this century of between 16 and 30 mmol m⁻³ (RCP8.5 “business as usual” scenario; Wakelin et al. (2020) and significant areas of
415 the NW European shelf are expected to be vulnerable to oxygen deficiency (Ciavatta et al., 2016; Wakelin et al., 2020). While these modelled DO reductions are broadly consistent with our findings, our suggestion that most of the future changes are caused by temperature-driven changes in metabolic rates is counter to recent modelling (Wakelin et al., 2020). Modelled



projections of DO show the strongest ecosystem impacts arising from changes in net primary production (netPP). Generally, changes in netPP are driven by changes in nutrient distributions, and netPP affects the amount of detrital organic material supplied to the bottom water community of bacteria. We have not considered changes in netPP and our observation-based measures of DO reduction rates have the advantage of not requiring any assumptions around detritus characteristics and the proportion of netPP that is transported below the thermocline. So, our observational approach is necessarily simple while models can incorporate a much broader suite of biogeochemical and physical processes. However, if we are confident in our estimate of microbial respiration rates and the Q_{10} parameterisation of their responses to a 2°C temperature change, then our suggestion that metabolic rate changes are greater than changes in oxygen solubility should be robust. Our results therefore highlight the need for better constraints on bottom water metabolic rates and a deeper understanding of how wind-driven mixing events may change in a warmer climate.

Data availability

The CTD observational data from the UK Shelf Sea Biogeochemistry programme used in this study are available at the British Oceanographic Data Centre (BODC): <https://www.bodc.ac.uk/resources/inventories/edmed/report/6368/>. ERA5 reanalysis wind speed data are available from the Copernicus Climate Change Service: <https://doi.org/10.24381/cds.adbb2d47>.

Author contribution

XM was responsible for conceptualization, data curation, formal analysis, investigation, methodology, visualization, and writing the original draft. CM contributed to conceptualization, supervision, and review and editing of the manuscript. JW contributed to data curation and review and editing of the manuscript. JS was responsible for conceptualization, methodology, supervision, visualization, and review and editing of the manuscript.

Competing interests

The authors declare that they have no conflict of interest.

Acknowledgements

Our thanks to the crews of the RRS Discovery and RRS James Cook, and technical support from the UK National Marine Facilities, during the UK Shelf Sea Biogeochemistry research programme.

Financial support



This research has been supported by the Natural Environment Research Council, UK Shelf Sea Biogeochemistry research programme (grant no. NE/K002007/1).

445 **References**

- Adams, K. A., Barth, J. A., and Chan, F.: Temporal variability of near-bottom dissolved oxygen during upwelling off central Oregon, *Journal of Geophysical Research: Oceans*, 118, 4839-4854, 2013.
- Barth, J. A., Pierce, S. D., Carter, B. R., Chan, F., Erofeev, A. Y., Fisher, J. L., Feely, R. A., Jacobson, K. C., Keller, A. A., and Morgan, C. A.: Widespread and increasing near-bottom hypoxia in the coastal ocean off the United States Pacific Northwest, *Scientific Reports*, 14, 3798, 2024.
- 450 Bendtsen, J., Hilligsøe, K. M., Hansen, J. L., and Richardson, K.: Analysis of remineralisation, lability, temperature sensitivity and structural composition of organic matter from the upper ocean, *Progress in Oceanography*, 130, 125-145, 2015.
- Breitburg, D.: Effects of hypoxia, and the balance between hypoxia and enrichment, on coastal fishes and fisheries, *Estuaries*, 25, 767-781, 2002.
- 455 Breitburg, D. L., Grégoire, M., and Isensee, K.: The ocean is losing its breath: Declining oxygen in the world's ocean and coastal waters, *IOC-UNESCO137*, 40, 2018.
- Brewer, P. G. and Peltzer, E. T.: Depth perception: the need to report ocean biogeochemical rates as functions of temperature, not depth, *Philosophical Transactions of the Royal Society A: Mathematical, Physical and Engineering Sciences*, 375, 2017.
- Burchard, H. and Rippeth, T. P.: Generation of bulk shear spikes in shallow stratified tidal seas, *Journal of Physical Oceanography*, 39, 969-985, 2009.
- 460 Ciavatta, S., Kay, S., Saux-Picart, S., Butenschön, M., and Allen, J.: Decadal reanalysis of biogeochemical indicators and fluxes in the North West European shelf-sea ecosystem, *Journal of Geophysical Research: Oceans*, 121, 1824-1845, 2016.
- Diaz, R. J. and Rosenberg, R.: Spreading dead zones and consequences for marine ecosystems, *Science*, 321, 926-929, 2008.
- García-Martín, E. E., Daniels, C. J., Davidson, K., Davis, C. E., Mahaffey, C., Mayers, K. M., McNeill, S., Poulton, A. J., Purdie, D. A., and Tarran, G. A.: Seasonal changes in plankton respiration and bacterial metabolism in a temperate shelf sea, *Progress in Oceanography*, 177, 101884, 2019.
- 465 Greenwood, N., Parker, E. R., Fernand, L., Sivyer, D. B., Weston, K., Painting, S. J., Kröger, S., Forster, R. M., Lees, H. E., Mills, D. K., and Laane, R. W. P. M.: Detection of low bottom water oxygen concentrations in the North Sea; implications for monitoring and assessment of ecosystem health, *Biogeosciences*, 7, 1357-1373, 10.5194/bg-7-1357-2010, 2010.
- 470 Große, F., Greenwood, N., Kreuz, M., Lenhart, H.-J., Machoczek, D., Pätsch, J., Salt, L., and Thomas, H.: Looking beyond stratification: a model-based analysis of the biological drivers of oxygen deficiency in the North Sea, *Biogeosciences*, 13, 2511-2535, 2016.
- Hersbach, H., de Rosnay, P., Bell, B., Schepers, D., Simmons, A., Soci, C., Abdalla, S., Alonso-Balmaseda, M., Balsamo, G., and Bechtol, P.: Operational global reanalysis: progress, future directions and synergies with NWP, 2018.



- 475 Hicks, N., Ubbara, G., Silburn, B., Smith, H. E., Kröger, S., Parker, E., Sivyer, D., Kitidis, V., Hatton, A., and Mayor, D.:
Oxygen dynamics in shelf seas sediments incorporating seasonal variability, *Biogeochemistry*, 135, 35-47, 2017.
- Holt, J., Wakelin, S., Lowe, J., and Tinker, J.: The potential impacts of climate change on the hydrography of the northwest
European continental shelf, *Progress in Oceanography*, 86, 361-379, 2010.
- Hopkins, J. E., Palmer, M. R., Poulton, A. J., Hickman, A. E., and Sharples, J.: Control of a phytoplankton bloom by wind-
480 driven vertical mixing and light availability, *Limnology and Oceanography*, 66, 1926-1949, 2021.
- Hull, T., Johnson, M., Greenwood, N., and Kaiser, J.: Bottom mixed layer oxygen dynamics in the Celtic Sea,
Biogeochemistry: An International Journal, 1, 10.1007/s10533-020-00662-x, 2020.
- Kemp, W. M., Sampou, P., Garber, J., Tuttle, J., and Boynton, W.: Seasonal depletion of oxygen from bottom waters of
Chesapeake Bay: roles of benthic and planktonic respiration and physical exchange processes, *Marine Ecology Progress Series*,
485 137-152, 1992.
- Laufkötter, C., John, J. G., Stock, C. A., and Dunne, J. P.: Temperature and oxygen dependence of the remineralization of
organic matter, *Global Biogeochemical Cycles*, 31, 1038-1050, 2017.
- Lefevre, D., Bentley, T., Robinson, C., and Blight, S.: The temperature response of gross and net community production and
respiration in time-varying assemblages of temperate marine micro-plankton, *Journal of Experimental Marine Biology and*
490 *Ecology*, 184, 201-215, 1994.
- Levin, L., Ekau, W., Gooday, A., Jorissen, F., Middelburg, J., Naqvi, S., Neira, C., Rabalais, N., and Zhang, J.: Effects of
natural and human-induced hypoxia on coastal benthos, *Biogeosciences*, 6, 2063-2098, 2009.
- Lincoln, B., Rippeth, T., and Simpson, J.: Surface mixed layer deepening through wind shear alignment in a seasonally
stratified shallow sea, *Journal of Geophysical Research: Oceans*, 121, 6021-6034, 2016.
- 495 Mahaffey, C., Hull, T., Hunter, W., Greenwood, N., Palmer, M., Sharples, J., Wakelin, S., and Williams, C.: Climate change
impacts on dissolved oxygen concentration in marine and coastal waters around the UK and Ireland, *MCCIP Science Review*,
2, 2023.
- Okubo, A.: Oceanic diffusion diagrams, *Deep Sea Research and Oceanographic Abstracts*, 18, 789-802, 10.1016/0011-
7471(71)90046-5, 1971.
- 500 Oschlies, A., Brandt, P., Stramma, L., and Schmidtko, S.: Drivers and mechanisms of ocean deoxygenation, *Nature*
Geoscience, 11, 467-473, 2018.
- Palmer, M. R., Inall, M. E., and Sharples, J.: The physical oceanography of Jones Bank: A mixing hotspot in the Celtic Sea,
Progress in Oceanography, 117, 9-24, 2013.
- Palmer, M. R., Rippeth, T. P., and Simpson, J. H.: An investigation of internal mixing in a seasonally stratified shelf sea,
505 *Journal of Geophysical Research: Oceans*, 113, 2008.
- Queste, B. Y., Fernand, L., Jickells, T. D., and Heywood, K. J.: Spatial extent and historical context of North Sea oxygen
depletion in August 2010, *Biogeochemistry*, 113, 53-68, 2013.



- Rippeth, T., Shen, S., Lincoln, B., Scannell, B., Meng, X., Hopkins, J., and Sharples, J.: The deepwater oxygen deficit in stratified shallow seas is mediated by diapycnal mixing, *Nature Communications*, 15, 3136, 2024.
- 510 Rovelli, L., Dengler, M., Schmidt, M., Sommer, S., Linke, P., and McGinnis, D. F.: Thermocline mixing and vertical oxygen fluxes in the stratified central North Sea, *Biogeosciences*, 13, 1609-1620, 2016.
- Ruiz-Castillo, E., Sharples, J., and Hopkins, J.: Wind-driven strain extends seasonal stratification, *Geophysical Research Letters*, 46, 13244-13252, 2019.
- Sarma, V., Rao, G., Viswanadham, R., Sherin, C., Salisbury, J., Omand, M. M., Mahadevan, A., Murty, V., Shroyer, E. L.,
515 and Baumgartner, M.: Effects of freshwater stratification on nutrients, dissolved oxygen, and phytoplankton in the Bay of Bengal, *Oceanography*, 29, 222-231, 2016.
- Schmidtko, S., Stramma, L., and Visbeck, M.: Decline in global oceanic oxygen content during the past five decades, *Nature*, 542, 335-339, 2017.
- Seguro, I., Marca, A. D., Painting, S. J., Shutler, J. D., Suggett, D. J., and Kaiser, J.: High-resolution net and gross biological
520 production during a Celtic Sea spring bloom, *Progress in Oceanography*, 177, 101885, 2019.
- Sharples, J., Holt, J., and Dye, S. R.: Impacts of climate change on shelf sea stratification, *MCCIP Science Review*, 2013, 67-70, 2013.
- Sharples, J., Holt, J., and Wakelin, S.: Impacts of climate change on shelf sea stratification, relevant to the coastal and marine environment around the UK, *MCCIP Science Review 2020*, 103-115, 2020.
- 525 Sharples, J., Mayor, D. J., Poulton, A. J., Rees, A. P., and Robinson, C.: Shelf Sea Biogeochemistry: Nutrient and carbon cycling in a temperate shelf sea water column, 2019.
- Sharples, J., Moore, M. C., Rippeth, T. P., Holligan, P. M., Hydes, D. J., Fisher, N. R., and Simpson, J. H.: Phytoplankton distribution and survival in the thermocline, *Limnology and Oceanography*, 46, 486-496, 2001.
- Sharples, J., Tweddle, J. F., Mattias Green, J., Palmer, M. R., Kim, Y.-N., Hickman, A. E., Holligan, P. M., Moore, C. M.,
530 Rippeth, T. P., and Simpson, J. H.: Spring-neap modulation of internal tide mixing and vertical nitrate fluxes at a shelf edge in summer, *Limnology and Oceanography*, 52, 1735-1747, 2007.
- Tweddle, J. F., Sharples, J., Palmer, M. R., Davidson, K., and McNeill, S.: Enhanced nutrient fluxes at the shelf sea seasonal thermocline caused by stratified flow over a bank, *Progress in Oceanography*, 117, 37-47, 10.1016/j.pocan.2013.06.018, 2013.
- 535 Wakelin, S. L., Artioli, Y., Holt, J. T., Butenschön, M., and Blackford, J.: Controls on near-bed oxygen concentration on the Northwest European Continental Shelf under a potential future climate scenario, *Progress in Oceanography*, 187, 102400, 2020.
- Wihsgott, J. U., Sharples, J., Hopkins, J. E., Woodward, E. M. S., Hull, T., Greenwood, N., and Sivyer, D. B.: Observations of vertical mixing in autumn and its effect on the autumn phytoplankton bloom, *Progress in Oceanography*, 177, 102059, 2019.
- 540 Williams, C., Sharples, J., Mahaffey, C., and Rippeth, T.: Wind-driven nutrient pulses to the subsurface chlorophyll maximum in seasonally stratified shelf seas, *Geophysical Research Letters*, 40, 5467-5472, 2013.

<https://doi.org/10.5194/egusphere-2026-3505>

Preprint. Discussion started: 25 June 2026

© Author(s) 2026. CC BY 4.0 License.



Williams, C., Davis, C., Palmer, M., Sharples, J., and Mahaffey, C.: The three Rs: Resolving respiration robotically in shelf seas, *Geophysical Research Letters*, 49, e2021GL096921, 2022.

Winkler, L. W.: Die bestimmung des im wasser gelösten sauerstoffes, *Berichte der deutschen chemischen Gesellschaft*, 21, 545 2843-2854, 1888.

Woolf, D. and Wolf, J.: Impacts of climate change on storms and waves, *MCCIP Science Review*, 2013, 20-26, 2013.